The Journal of Experimental Biology 209, 590-598
Published by The Company of Biologists 2006
doi:10.1242/jeb.02034

Dynamics of the aerial maneuvers of spinner dolphins

Frank E. Fish[1,*], Anthony J. Nicastro[2] and Daniel Weihs[3]

[1]*Department of Biology and* [2]*Department of Physics, West Chester University, West Chester, PA 19383, USA and* [3]*Faculty of Aerospace Engineering, Technion, Israel Institute of Technology, Haifa 32000, Israel*

*Author for correspondence (e-mail: ffish@wcupa.edu)

Accepted 12 December 2005

Summary

The spinner dolphin (*Stenella longirostris*) performs spectacular leaps from the water while rotating around its longitudinal axis up to seven times. Although twisting of the body while airborne has been proposed as the mechanism to effect the spin, the morphology of the dolphin precludes this mechanism for the spinning maneuver. A mathematical model was developed that demonstrates that angular momentum to induce the spin was generated underwater, prior to the leap. Subsurface corkscrewing motion represents a balance between drive torques generated by the flukes and by hydrodynamic forces at the pectoral fins, and resistive torques, induced by the drag forces acting on the rotating control surfaces. As the dolphin leaps clear of the water, this balance is no longer maintained as the density of the air is essentially negligible, and a net drive torque remains, which permits the dolphin's rotation speed to increase by as much as a factor of three for a typical specimen. The model indicates that the high rotation rates and orientation of the dolphin's body during re-entry into the water could produce enough force to hydrodynamically dislodge unwanted remoras.

Key words: spinner dolphin, *Stenella longirostris*, spinning, swimming, maneuver, angular momentum.

Introduction

Many cetaceans perform aerial maneuvers, in which they leap from the water into the air. These maneuvers, including porpoising, leaping and breaching, are associated with breathing patterns, swimming energetics, play, hunting, removal of ectoparasites, territoriality and acoustic communication (Au and Weihs, 1980; Hui, 1989; Pryor and Norris, 1991; Norris et al., 1994; Weihs, 2002; Weihs, 2004). By launching an entire body weighing 40 000 kg out of the water when breaching, humpback whales (*Megaptera novaeangliae*) may be considered highly acrobatic (Edel and Winn, 1978; Winn and Reichley, 1985). However, greater agility is observed in the aerial leaping of spinner dolphins, *Stenella longirostris* and *Stenella clymene*.

The 'trademark' aerial behavior of spinner dolphins is a twisting leap (Hester et al., 1963; Norris and Dohl, 1980; Norris et al., 1994). These dolphins turn around their longitudinal axis, rotating as many as seven times when clear of the water (Hester et al., 1963; Leatherwood et al., 1988; Norris et al., 1994). A single animal can perform up to 14 successive spinning leaps, with each less vigorous than the preceding leap (Perrin and Gilpatrick, 1994; Perrin, 2002). Heights of 3 m have been attained by the spinning dolphins and an airborne time of 1.25 s was measured (Hester et al., 1963; Perrin and Gilpatrick, 1994). Spinning is most frequently observed in slowly swimming groups and less frequently in fast-swimming animals (Hester et al., 1963). Although both *S. longirostris* and *S. clymene* can perform spinning leaps, *S. longirostris* displays the more spectacular spinning behaviors.

The question remains, how are spinner dolphins able to execute their spectacular twisting leaps? Although uncertain of the exact mechanism because of the inability to observe an animal above and below the water simultaneously, Norris and Dohl (1980) and Norris et al. (1994) considered that a dolphin could effect a spin by flexing its tailstock and throwing the airborne part of its body into a twisted pattern. This mechanism for spinning, however, seems highly implausible. Dolphins have limited twisting ability (58–88°; Fish, 2002) about the longitudinal axis due to skeletal modifications (Slijper, 1962; Rommel and Reynolds, 2002). Some twisting is permitted at the tail, but any twisting negates the ability of the dolphin to produce swimming motions necessary to leap clear of the water (Fish, 2002). In addition, the twisting motions are too small and the distribution of mass is too close to the central axis of the body to produce sufficient torque to provide the angular momentum and rotate the body.

Norris et al. (1994) published a series of excellent time-lapse drawings illustrating a typical aerial spin, wherein a dolphin made three complete rotations before falling back into the water. Thus, while airborne, the spinner dolphin possessed a net angular momentum. If a dolphin were to emerge from the surface with no initial angular momentum, once airborne no

means exist for a net torque to be exerted on the animal to produce the observed spin. Twists and flexures of the body can certainly affect orientation, much as a cat dropped initially upside down can reorient itself by creating internal torques, so that it falls feet first. In the case of a falling cat, however, both the initial and final states have no net angular momentum (Frohlich, 1980). Such reorientation is noted in some of the concluding motions of a dolphin's spin when an animal that has just executed a nearly vertical leap essentially falls back laterally into the water. The spin itself, though, is marked by complete rotations about the animal's longitudinal axis.

In order to account for the net angular momentum of an airborne spinner dolphin, the subsurface motion must also be characterized as possessing a net angular momentum. Corkscrewing or barrel-roll behavior is a typical maneuver of dolphins, in which the animal rolls while rectilinearly swimming (Fish, 2002). A corkscrewing dolphin rotating with a constant angular velocity has no net torque acting on it. It's motion is compounded by a rectilinear propelled motion along the animal's path and a uniform rotational motion around this path. The rotational motion generates large drag forces on the control surfaces (e.g. flippers, fin, flukes). The torques produced by these drag forces are offset by additional torques generated by the powered motion of the animal, achieving a uniform rate of rotation.

In the absence of a net external torque, the angular momentum remains constant. A dolphin with a moment of inertia, I, and corkscrewing at constant angular velocity, ω, about its longitudinal axis possesses an angular momentum $L=I\omega$. A constant ω implies that I is constant and therefore all the torques on the corkscrewing dolphin balance. Thus, the resistive torques, which are produced by drag forces on control surfaces, are equal and opposite to drive torques generated by the flukes and pectoral flippers, neglecting the smaller torque on the body due to the viscous resistance to the turning motion. We shall refer to this as Dynamic Balance Condition 1. In addition, video of corkscrewing dolphins does not show any systematic torsion along the longitudinal axis. Any imbalance between the hydrodynamic drive torque at the pectoral flippers and the drive torque produced by the flukes would cause the spin rate of the anterior half of the animal to differ from the posterior half, resulting in a continual twist. The lack of such a systematic torsion in the body while corkscrewing implies that the animal balances the hydrodynamic drive torque at the canted pectoral flippers and the drive torque produced at the flukes. We shall refer to this at Dynamic Balance Condition 2.

Note that an imbalance is necessary if the animal changes its rotational rate while corkscrewing. The drag torque at the pectoral flippers, dorsal fin and flukes produced by the corkscrewing motion all vary with respect to relative size and the angular speed of the corkscrewing motion. In a spinning maneuver, as the animal emerges out of the water from a corkscrew precursor, the dolphin sheds resistive torques as the flippers, dorsal fin and flukes successively leave the water. In addition, a driving torque is lost as the flippers emerge. We shall show in the following analysis, however, that the driving torque produced by the flukes is large compared to the small resistive torques remaining, and the angular speed of the dolphin increases accordingly. In the following we show that this model satisfactorily describes the observed motions of spinner dolphins, both while in their submerged corkscrew-swimming and in their aerial spinning maneuvers.

Model for aerial spinning

Typical specimens of *S. longirostris* possess characteristics listed in Table 1. An important factor in characterizing the dynamics of a dolphin is its moment of inertia. In our model, the total moment of inertia, I_{total}, is calculated by summing the contributions from the body, pectoral fins, dorsal fin and flukes:

$$I_{\text{total}} = I_{\text{body}} + I_{\text{flippers}} + I_{\text{fin}} + I_{\text{flukes}} . \quad (1)$$

Each individual moment is determined from the relation:

$$I = \int R^2 \mathrm{d}M_{\text{b}} , \quad (2)$$

where the integration is over each control surface (Fig. 1), and I_{body} is taken to be that of an ellipsoid whose long axis equals the total length of the dolphin and with equal minor axes (giving circular cross-sections), which are equal to the radius at the axilla. With this approximation, $I_{\text{body}}=2/5M_{\text{b}}R^2$, where M_{b} is the dolphin's mass and R is the maximum radius of the

Table 1. *Body characteristics* of a spinner dolphin*

Body	
Total length	1.82 m
Mass	65 kg
Girth at axilla	0.82 m
Corresponding radius	0.13 m
Average radius	0.10 m
Maximum radius (at dorsal fin)	0.15 m
Conformation of pectoral flipper – parallelogram, 45° rake	
Length	0.28 m
Width	0.08 m
Model area	0.022 m^2
Model area (Ψ=30°)	0.019 m^2
Conformation of dorsal fin – isosceles triangular	
Height	0.16 m
Width at base	0.42 m
Model area	0.34 m^2
Conformation of fluke – right triangular	
Width	0.32 m
Depth	0.11 m
Model area	0.25 m^2

Masses and dimensions are used to model the aerial spinning dynamics of spinner dolphins (*Stenella longirostris*).

*Dimensions are based on data from average values (Perrin and Gilpatrick, 1994) and scaled photographs of appendages for a related species (*Stenella clymene*; NMNH504408).

Ψ is the angle that the pectoral flippers are canted to the water flow.

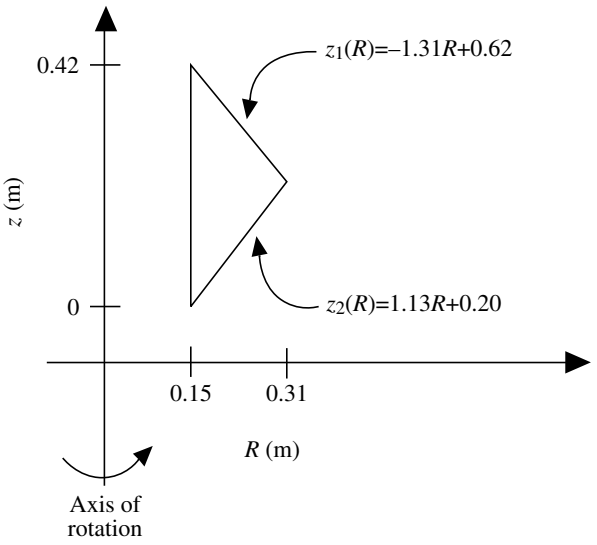

Fig. 1. Illustration of the method by which the moment of inertia of a control appendage is calculated. This figure shows an example using the dorsal fin. The vertical z-axis represents the axis of rotation, which runs longitudinally through the center of the dolphin. The horizontal R-axis measures the distance from the axis of rotation. In this example for the model dorsal fin, an isosceles triangular shape is adopted whose height is 0.16 m and base is 0.42 m in length, and is 0.15 m from the axis of rotation. The equations of the canted edges of the dorsal fin are indicated. For our calculations, the area mass density of the control surfaces was taken to be 30 kg m^{-2} (F. E. Fish, unpublished data).

dolphin (Table 1). The differential mass dM_b is a function of the particular control appendage's size, mass, geometry, relative position and orientation with respect to the dolphin's body. For the model dolphin represented in Table 1, I_{body}, $I_{flippers}$, I_{fin} and I_{flukes} are 0.585, 0.069, 0.043 and 0.007 kg m^2, respectively, with I_{total}=0.704 kg m^2 (see Appendix for a detailed example calculation). Using more realistic shapes to calculate the moment of inertia of the body and control appendages is not expected to alter I_{total} substantially enough to affect the character of our results.

A spinner dolphin preparing to execute a spinning leap from a subsurface corkscrew precursor will have an angular momentum equal to $I\omega_A$, where I=I_{total} from above and ω_A is the initial angular speed prior to a leap. ω_A is assumed to be 1–2 revolutions per second around the animal's longitudinal axis, based on observations of corkscrewing by captive dolphins (F. E. Fish, unpublished observations). As the dolphin emerges from water, successive body parts become airborne. In so doing, resistive torques are eliminated, but so are drive torques. The dynamics of the spinning maneuver are determined by the time sequence of these changes.

For the purposes of this model, four stages characterize the emergence of the dolphin performing a spinning maneuver: A, animal goes from completely submerged to just before pectoral fins begin to emerge; B, pectoral fins emerge to just prior to the emergence of the dorsal fin; C, the dorsal fin emerges to the time just prior to the flukes emerge; D, the flukes emerge and the animal is freely spinning in a leap. We make the conservative assumption that the animal's angular momentum while submerged is constant because the spin rate is constant, but both will change in response to whatever net torque remains acting on the animal in stages B and C.

Resistive torques

We determine the resistive torques produced by a submerged control appendage by the vector relation τ=**r**×**F**, where **F** is the vector drag force associated with each appendage and **r** is the vector moment arm of **F**. Because the corkscrew motion can be decomposed into a rectilinear propelled motion along the animal's path and a uniform rotational motion around this path, this expression can be simplified to τ=rF. Thus,

$$\tau = r(\tfrac{1}{2}\rho A C v^2) = r(\tfrac{1}{2}\rho A C \omega_A^2 r^2) , \quad (3)$$

where C is a dimensionless coefficient and v is tangential speed. The differential amount of resistive torque produced by an element of the appendage of area dA a distance r away from the rotational axis is:

$$d\tau = r dF = r(\tfrac{1}{2}\rho dA C \omega_A^2 r^2) = \tfrac{1}{2}\rho C \omega_A^2 r^3 dA . \quad (4)$$

Now, to determine the resistive torque acting on an appendage, the above expression must be integrated over the surface area of the appendage. Leaving ω_A as a free parameter and taking C=1.2 (Potter and Foss, 1975), ρ=1025 kg m^{-3}, the resistive torque (in N m) for each control appendage is found to be:

$$\tau_{pectoral\ fins} = 0.35\omega_A^2 , \quad (5a)$$

$$\tau_{dorsal} = 0.19\omega_A^2 , \quad (5b)$$

$$\tau_{flukes} = 0.02\omega_A^2 . \quad (5c)$$

The total resistive torque experienced by a submerged, corkscrewing dolphin is therefore:

$$\tau_{total} = 0.56\omega_A^2 . \quad (6)$$

Because while submerged and corkscrewing ω_A is constant, the total drive torque must compensate for this resistive torque according to Dynamic Balance Condition 1. Additionally, in our model the dolphin possesses only two sources of drive torques that counteract the effects of drag forces producing resistive torques, while corkscrewing: one at the pectoral flippers and the other at the flukes. Furthermore, according to Dynamic Balance Condition 2, the lack of a systematic torsion in a corkscrewing dolphin implies that the total drive torque must be split equally between the hydrodynamic torques generated at the pectoral flippers and the torque created by the flukes. Thus,

$$\tau_{drive,\ pectoral\ fin} = \tau_{drive,\ flukes} = 0.28\omega_A^2 . \quad (7)$$

As a spinner dolphin emerges from the water from a corkscrew precursor, the balance between resistive torques and drive torques is disturbed, and because the pectoral fins are the first control appendages to emerge and also represent a net loss of resistive torque (τ=0.35ω_A^2–0.28ω_A^2), the animal begins to spin faster.

The ultimate spin rate achievable by the animal now depends on the time between when the pectoral fins emerge and when the flukes finally clear the water and can no longer produce a torque. This time, in turn, is dependent upon the swim speed. Also of importance are the relative positions and separations along the longitudinal axis of the pectoral fins, the dorsal fin and the flukes. To examine the consequences of our model, we define a nominal case, based on measurements from a specimen of *Stenella clymene* (NMNH 504408), whose total length is 1.86 m and has the pectoral fins and dorsal fin separated by 0.65 m and a distance of 0.91 m between the dorsal fin and the fluke notch (Table 1).

At any stage during the spinner's emergence from the water, the net torque on the animal determines the changes in its spin rate:

$$\tau_{net} = \frac{dL}{dt} = I\,\frac{d\omega}{dt} = I\,\frac{\Delta\omega}{\Delta t}\,. \quad (8)$$

Therefore,

$$\Delta\omega = \frac{\tau_{net}\Delta t}{I} = \frac{\tau_{net}\dfrac{\Delta x}{v_s}}{I}\,, \quad (9)$$

where v_s is the swim speed and Δx is the distance between any two points on the animal. τ_{net} is the net torque acting over the time interval Δt while a distance Δx on the animal emerges from the water. $\Delta\omega$ is the increase in angular speed due to the action of τ_{net}.

A dolphin that launches itself with an escape velocity of v_s at an initial angle θ_o with respect to the surface, will have an airborne time of $t=(2v_s\sin\theta_o)/g$, where g is the acceleration of gravity, 9.8 m s^{-2}. The number of complete spins executed by a dolphin with vertical emergence rotating with an angular speed of ω_D in stage D is therefore:

$$N = \frac{\omega_D}{2\pi}\,t\,. \quad (10)$$

ω_D can be related back to the initial angular speed ω_A by means of Eqn 8 and 9. The result is:

$$\frac{\pi N g}{v_s} = \omega_A + \frac{\tau_{net,B}\Delta x_B}{v_s I} + \frac{\tau_{net,C}\Delta x_C}{v_s I} \quad (11a)$$

or

$$= \omega_A + \frac{0.07\omega_A^2\Delta x_B}{v_s I} + \frac{0.26\omega_A^2\Delta x_C}{v_s I}\,, \quad (11b)$$

where Δx_B is the distance between the pectoral fins and the dorsal fin (0.65 m), relevant to the stage B motion, and Δx_C is the distance between the dorsal fin and the flukes (0.91 m), relevant to the stage C motion.

In Eqn 11, we can therefore relate the initial angular speed, the swim speed, and the number of complete spins possible for the animal to execute. We note that from the results in Table 2, a dolphin with the relatively high swim speed of 4 m s^{-1} can execute up to 6 complete spins in the time it is airborne. This result is consistent with video recordings of dolphins in the wild completing 7 spins, but with an emergent angle of about 50°.

Table 2. *Development of the angular velocity ω for the model spinner dolphin with vertical emergence at different swimming velocities*

	v_s=2 m s^{-1}		v_s=4 m s^{-1}	
	ω_A=1 rev s^{-1}=6.3 rad s^{-1}		ω_A=2 rev s^{-1}=12.6 rad s^{-1}	
Spin stage	τ_{net} (N m)	ω (rad s^{-1})	τ_{net} (N m)	ω (rad s^{-1})
A	0	6.3	0	12.6
B	2.8	7.6	11.1	17.7
C	10.3	10.9	41.1	31.0
D	0	10.9	0	31.0

Spin stage – for definitions, see text and Fig. 4.

The values of ω quoted in the table are for the end of the time interval comprising each stage.

Note, too, in Eqn 11a,b, that the moment of inertia (I) of the dolphin appears in the denominator of the two terms, which represent the increase in the spin rate of the dolphin as it emerges from water into air. Thus, animals with smaller moments of inertia and a slimmer body shape are better suited to spinning. The resistive torques, however, appear in the numerator, which favor larger appendages.

Materials and methods

Data to test the model were obtained from a video recording of aerial maneuvers by spinner dolphins (*Stenella longirostris* Gray 1828) supplied by Natural History New Zealand (NHNZ, Dunedin, NZ). Dolphins were filmed at the Bay of Dolphins in the Fernando de Noronha Archipelago, which is located 345 km east of the Brazilian mainland.

Forty-five aerial maneuvers were analyzed. The video was examined frame-by-frame with a Panasonic AG-7300 video recorder and Panasonic CT-2600M monitor. As framing rate varied and there were no scale metrics in the video, data were restricted to counts of video frames and numbers of body rotations. Initial rotation of the dolphin (stage A) was measured as the number of frames to complete a half rotation (F_A) starting from the moment the rostrum emerged through the water surface. Aerial rotation (stage D) was measured as the number of frames to complete one full rotation once the dolphin was completely airborne (F_D). Difference in rotation rates between stage A and stage D was expressed as a Spin Index, according to the ratio $(2F_A)/F_D$. The number of aerial spins was counted as the rotations of the body once the flukes had cleared the water surface until the body impacted the water.

Results

The spinner dolphins observed in the video performed aerial maneuvers similar to previous descriptions (Hester et al., 1963;

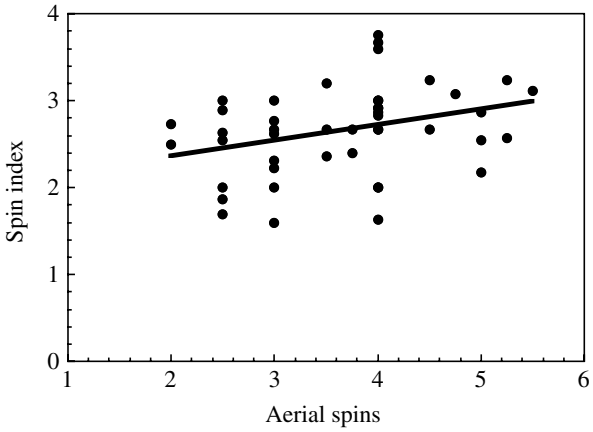

Fig. 2. Regression of the spin index against the number of aerial spins by spinner dolphins. The regression line is described by the equation: spin index=2.00+0.18 aerial spins.

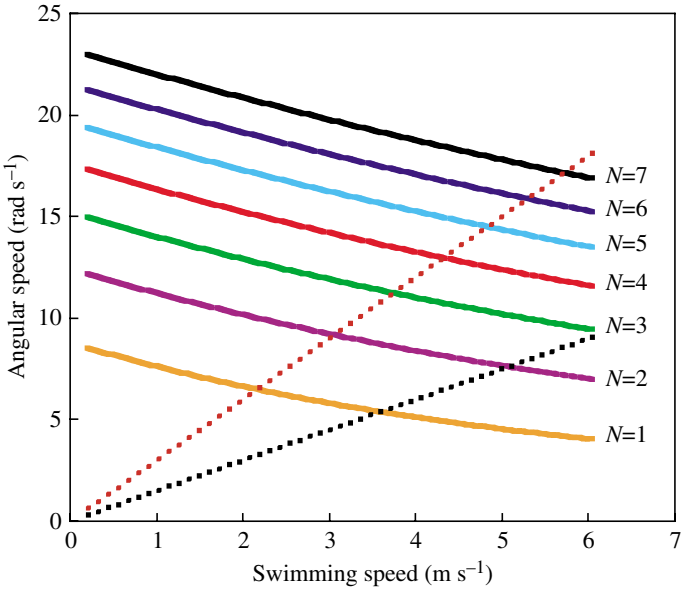

Fig. 3. Relationship between the angular speed (ω_A) while corkscrewing necessary to execute various numbers of complete spins (N) over a range of swimming speeds (v_s). The dotted diagonal lines indicate a realistic approximation of the spinning performance of the dolphin, where the angular speed is directly proportional to the swim speed (i.e. $\omega_A=\theta_R v_s$). The black dotted line is based on the observation of spinning rate from *Lagenorhynchus obliquidens* of θ_R=1.5 rad m^{-1}. The red dotted line is for θ_R=3 rad m^{-1} in order to achieve seven aerial spins, which is the maximum number of spins observed for *Stenella longirostris* (Norris et al., 1994).

Norris and Dohl, 1980; Norris et al., 1994). The dolphin emerged through the water surface, rostrum first. The body was observed to rotate as the body moved upward. The rate of rotation appeared to increase once the dolphin was completely airborne. In the air, the dolphin rose to its maximum leap height and then fell back to the water, executing a parabolic trajectory. In addition to the axial spin and ballistic movement, the body would typically rotate to present the lateral aspect of the body to the water surface upon re-entry.

The total number of aerial spins ranged from 2 to 5.5 (mean ± s.d.=3.7±0.9). The spin index had a mean of 2.7±0.5 and ranged from 1.6 to 3.8. A regression of the relationship between numbers of aerial spins and spin index (Fig. 2; KaleidaGraph 3.0) showed a significant positive correlation (r=0.32; d.f.=43; P<0.05).

Table 2 presents four stages in the emergence of a spinner dolphin executing a spin maneuver and the corresponding net torque at each stage. The evolution of the animal's angular velocity is also shown for two different initial rates of rotation while submerged and for two different swim speeds.

The summarized results of the model are shown in Fig. 3. The number of complete spins is dependent on the relationship between the swim speed and angular speed while corkscrewing underwater. High numbers of aerial spins by dolphins are achieved with higher angular and swimming speeds compared to low spin numbers. With increasing swim speeds, more spins are possible for a given angular speed.

Discussion

The motion of the spinner dolphin performing aerial maneuvers is a combination of translational and rotational motion. The center of mass of the dolphin follows a ballistic trajectory, which is dependent on the escape velocity and escape angle. The aerial spin starts underwater by rotating the body around its longitudinal axis (Fig. 4). Underwater the dolphin produces drive torques, which compensate for the large resistive torques acting on the appendages. As the dolphin emerges in the leap, its hydrodynamic drive torque and resistive torque of the pectoral flippers vanishes, as does the resistive torque of the dorsal fin. The remaining drive torque produced by the flukes is larger than the resistive torque experienced by the flukes. The torque imbalance produces an acceleration that increases the dolphin's spin rate. After the dorsal fin emerges, the large drive torque generated by the flukes acts over the comparatively large time between when the dorsal fin emerges and the flukes leave the water. This results in an even greater increase in the spin rate (Fig. 4).

Actually, even if the underwater moments are not balanced, this does not change the model's validity, as the sudden decrease in resistive torque is the factor that produces the increase in spin rate. Lacking detailed underwater films, the existence, or non-existence, of a balance of moments underwater can only be checked *a posteriori* through the results. However, the fact that the spin number is much larger than one, and the correlation between spin number and forward speed indicates that the decrease in resistive moments due to water exit is a dominant, if not exclusive factor.

Spinning is enhanced also by the morphology of the spinner dolphin, which has a relatively slender body compared to other dolphins. The Fineness Ratio (FR) is an indicator of body slenderness and can be computed from length (l) and girth (G)

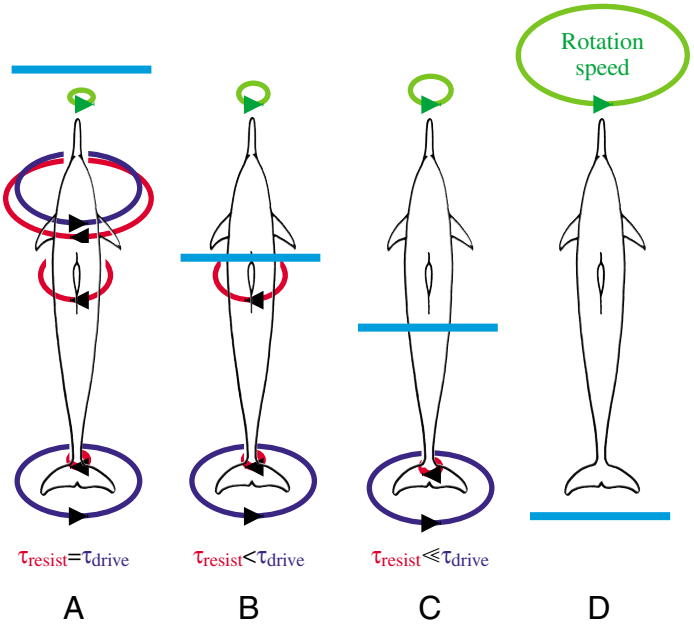

Fig. 4. Diagram summarizing the four stages of a spinning leap. (A) Animal is completely submerged while corkscrewing, (B) pectoral fins emerge, (C) the dorsal fin emerges, and (D) the flukes emerge and the animal is freely spinning while airborne. The relationship is shown between rotation speed of the dolphin body and resistive (red) and drive (blue) torques developed underwater. Arrowheads indicate the direction of the opposing torques. The surface of the water is indicated by the light blue line and the magnitude of the rotational speed by the size of the green ovals.

measurements as $FR=l/(G\pi)$. For 858 *Stenella longirostris* collected as Tuna purse-seine by-catch in the eastern Pacific Ocean (S. Chivers, unpublished data), mean *FR* was 6.34±0.45 (± s.d.). This value for *FR* is generally higher than for similarly sized dolphins (Fish et al., 2003). The more slender body morphology of spinner dolphins reduces the moment of inertia (*I*) and enhances spinning performance, in accordance with Eqn 11.

The typical behavior of spinner dolphins executing 3–6 rotations in the air is satisfactorily accounted for with corkscrewing precursors of 1–2 rev s^{-1}. These results are consistent with the observed achievable swimming speeds of spinner dolphins of 4.6 m s^{-1} (Au and Perryman, 1982). For a dolphin that launches itself at an angle with respect to the surface, its airborne time is $t=(2v_o\sin\theta_o)\boldsymbol{g}^{-1}$. A dolphin corkscrewing underwater at a rate of 2.7 rev s^{-1}, having a translational speed of 5.7 m s^{-1}, and emerging perpendicular to the water's surface, will be able to execute 7 complete spins in the one second it is airborne. Spinner dolphins are capable of reaching speeds up to 7.2 m s^{-1}, and a leap velocity of 6.1 m s^{-1} was calculated from a 1.25 s jump (Hester et al., 1963).

The mechanism for corkscrewing as the underwater precursor of the aerial spin has not been investigated. Twisting of the flukes during powered swimming may be constrained, although twisting of the flukes can occur rapidly during turning maneuvers (Fish, 2002). The dorsal fin is immobile and cannot aid in corkscrewing. The pectoral flippers are mobile and can effect the rotation of the body. Underwater observations of a Pacific striped dolphin *Lagenorhynchus obliquidens* horizontally swimming at 4.1 m s^{-1} while corkscrewing at 1 rev s^{-1} (6.3 rad s^{-1}) showed that the flippers were canted at an angle to the longitudinal body axis and axis of progression (Fig. 5). By having the flippers angled to the incident flow, lift is generated and directed to induce a turning moment.

A rotational performance coefficient θ_R is defined as $\theta_R=\omega_A/v_s$, whereby θ_R is the ratio of the initial rate of rotation to the animal's swim speed. It gives the amount of rotation the animal can effect per meter of distance traveled. The equation also expresses the intuitive notion that the angular speed while corkscrewing is directly proportional to the swim speed. Using the data above, $\theta_R=(6.3\text{ rad s}^{-1})/(4.1\text{ m s}^{-1})=1.5\text{ rad m}^{-1}$. θ_R is controlled by the animal and can vary from zero (swimming in

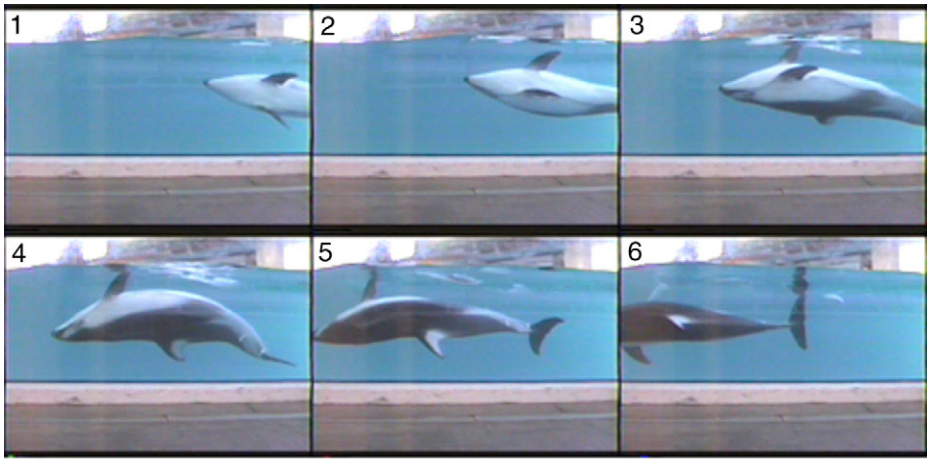

Fig. 5. Time sequence of photographs from video of the underwater corkscrewing motion of a Pacific striped dolphin (*Lagenorhynchus obliquidens*). The corkscrewing motion is characterized by a balance of the anterior drive torque at the pectoral flippers and the posterior drive torque produced at the flukes. Any anterior–posterior imbalance would generate a systematic, continual torsion of the anterior half with respect to the posterior half (Dynamic Balance Condition 2). This torsion would be indicated by a helical twisting in the dorsal/ventral line of coloration discontinuity. This sequence of images of the corkscrewing dolphin shows no discernable torsion in the body. This orientation demonstrates the balance in torques that the animal achieves in order to execute corkscrewing motion at a uniform rotational rate. A uniform rate of rotation around the longitudinal axis itself is indicative of a balance of resistive torques and drive torques (Dynamic Balance Condition 1). Image 6 shows the dorsal fin canted due to the resistive torque in rotational motion.

a straight line with no rotation) to some maximum value permitted by the morphology of the dolphin and regulated by the amount the pectoral flippers can be canted and how much the tailstock can be torsioned. Later we shall show that θ_R has an upper limit of approximately 3 rad m^{-1} for spinner dolphins.

No single factor is considered to be the reason for the aerial spinning behavior (Hester et al., 1963; Norris and Dohl, 1980; Norris et al., 1994). The various factors include leadership or dominance, alertness, acoustic communication, courtship display, defining positions of members in the school, and dislodging ectoparasites. The most notable ectoparasites are remoras and whalesuckers (order Perciformes, family Echeneidae). These fish display a hitchhiking behavior where they use a suction disc to attach to the body of a larger host (O'Toole, 2002). Echeneids are known to attach to cetaceans (Fertl and Landry, 1999; Guerrero-Ruiz and Urbán, 2000; O'Toole, 2002).

Hester et al. (1963) suggested that the aerial maneuvers executed by spinner dolphins are involved in the removal of remoras. Jumping by blacktip sharks *Carcharhinus limbatus* has been proposed as a means of dislodging attached echeneid sharksuckers *Echeneis naucrates* (Ritter, 2002; Ritter and Brunschweiler, 2003). Remoras are considered hydrodynamic parasites as they potentially disrupt the flow over the dolphin's body and add to the drag, although remoras can be beneficial in clearing parasites (Cressey and Lachner, 1970; Moyle and Cech, 1988; O'Toole, 2002). The sucking disc of remoras is a modified dorsal fin with slat-like transverse ridges, which are modified spines (Moyle and Cech, 1988). These spines may act as an irritatant (Ritter and Godknecht, 2000; Ritter, 2002) on the highly sensitive skin of the dolphin, particularly as drag increases on the remora with increased swimming speed of the dolphin. The integument of the dolphin is more richly innervated, more elaborate and more specialized than the skin of humans (Palmer and Weddell, 1964). Tactile sensitivity is high, with sensitivity equivalent to the skin of the human lips and fingers (Kolchin and Bel'kovich, 1973; Ridgway and Carder, 1990, 1993).

Norris et al. (1994) noted that approximately half the spinning dolphins that were observed in photographs showed one or more remoras attached to the body. Their sense, though, was that in free-swimming specimens, the frequency of attached remoras was far smaller than the 50% seen in photographs. As dolphins with and without remoras demonstrated spinning, Hester et al. (1963) rejected their original hypothesis, although Norris et al. (1994) still considered it a possibility.

The model presented above, however, can provide a mechanical test to evaluate if spinning has some potential benefit in the dislodgment of remora parasites. A spinner dolphin rotating at an intermediate rate of 30 rad s^{-1} (Table 2) will have a point on its body moving with a speed of $v=\omega R=3.0$ m s^{-1}. This corresponds to a centripetal acceleration of $a_c=\omega^2R=v^2/R$ of approximately 9 *g*. Thus, an attached remora experiences a force nine times its own weight at the point of attachment. Large specimens of remoras can be up to 1 m in length and have masses of approximately 10 kg (mass in kg=10×(length in m)^3; Webb, 1975). The question now arises, could one attach a 90 kg mass to the end of a remora and break its hold on a dolphin? Such a measurement has not been conducted, but the affirmative result seems plausible.

By executing spinning maneuvers, dislodgment of remoras is possible because during a spin, the majority of the remora's body, which is posterior of the attached pectoral fin (Fertl and Landry, 1999), has its longitudinal axis essentially oriented radially to the dolphin. When the dolphin re-enters the water with the attached remora nearly perpendicular to its skin surface, the impact and the large laterally directed drag forces potentially could dislodge any attached parasite. The drag force on a remora spun out radially can be estimated for a dolphin re-entering the water after a leap of 2 m in height. The speed of the dolphin on impact is approximately 6 m s^{-1}. The spin of the dolphin will have 0.4 m long remora, moving with a speed at its midpoint of about 7.5 m s^{-1} (Table 2). The relative speed of the remora with respect to the water's surface can be 13.5 m s^{-1}.

The drag force F_{drag} experienced by the remora can be estimated from $F_{drag}=0.5\rho A C_d v^2$, where C_d is the drag coefficient. As there is an attached portion of the remora about its head, which hydrodynamically interacts with the dolphin body surface, and an unattached portion, which is represented by the body posterior of the head and sucker, the drag is different between these portions. The total drag on the remora is the sum of the attached head and free body:

$$F_{drag} = F_{drag,head} + F_{drag,body} \quad (12a)$$

$$F_{drag} = 0.5\rho v^2(A_{head}C_{d,head}+A_{body}C_{d,body}) , \quad (12b)$$

where C_d is the drag coefficient in two-dimensional flow (i.e. based on projected surface area). $C_{d,head}$ is 0.09, based on a half streamline body in the presence of the ground (Hoerner, 1965), whereas $C_{d,body}$ is 1.2, based on a circular cylinder (Streeter, 1966).

The shark remora or sharksucker *Echeneis naucrates* was observed on spinner dolphins in Brazil (Fertl and Landry, 1999). A preserved sharksucker purchased from a commercial dealer had a mass of 139.7 g, and was 384 mm in total length with a maximum depth of 30 mm. The head and sucker comprised 24% of the total length. The lateral projected surface area of the head and sucker, 1320 mm^2 and of the body posterior of the sucker, 8497 mm^2. With these values, F_{drag} is approximately 960 N, which is approximately 700 times the remora's weight! Townsend (1915) found that 0.61 and 0.67 m long specimens of *E. naucrates* could lift pails of water weighing 93.4 and 107.9 N, respectively. The calculated F_{drag} that can be generated by the smaller remora in the present study is still 10.3 and 8.9 times greater than weights that the remoras were reported to support (Townsend, 1915). Thus if the spinning maneuvers of *S. longirostris* are intended to dislodge *E. naucrates*, the effect is achieved by flinging the remoras into a radial orientation so that drag forces on re-entering the water can laterally shear off the attached parasites.

The spin in air would be less effective at casting off remoras. The spinning maneuver is therefore more effective than simply leaping out of the water. In a leap, any attached remora would have its long axis parallel to the skin; therefore, the drag forces on the remora would be far smaller on re-entering the water and would be less likely to be dislodged. While aerial spinning maneuvers may not have developed specifically to remove ectoparasites like remoras, dynamically it is plausible that this proves to be an added benefit.

Appendix

Calculation of resistive torque on dorsal fin of model dolphin

As an illustration of our method of determining the resistive torque on any control surface in rotational motion, we consider the drag force acting on the dorsal fin. From Eqn 4, the resistive torque on any differential element of area dA of the dorsal fin a distance r from the axis of rotation will be $d\tau=\frac{1}{2}\rho C\omega_A^2 r^3 dA$. Consider an area element of width dr and of length $z_1(r)–z_2(r)$ on the model dorsal fin depicted in Fig. 1. Therefore, $d\tau=\frac{1}{2}\rho C\omega_A^2 r^3[z_1(r)–z_2(r)]dr$, which in this case yields

$$d\tau = \tfrac{1}{2}\rho C\omega_A^2 r^3[-2.625r+0.8136]dr = \tfrac{1}{2}\rho C\omega_A^2[-2.625r^4+0.8136r^3]dr .$$

To determine the total resistive torque, we integrate over the entire surface area of the dorsal fin from the base where it meets the body out to the tip, i.e. from r=0.15 m to r=0.31 m. Thus,

$$\tau = \tfrac{1}{2}\rho C\omega_A^2 \int_{r=0.15}^{r=0.31} [-2.625r^4+0.8136r^3]dr$$

$$= \tfrac{1}{2}\rho C\omega_A^2 \left[\frac{-2.625}{5} r^5 + \frac{0.8136}{4} r^4 \right]_{r=0.15}^{r=0.31}$$

$$= \tfrac{1}{2}(1025)(1.2)\omega_A^2(0.000312) .$$

Inserting appropriate values for ρ and C, evaluating the integral at its limits, and leaving ω_A as a free parameter, we obtain:

$$\tau = \tfrac{1}{2}(1025)(1.2)\omega_A^2(0.000312) = 0.19\omega_A^2 .$$

All quantities are in standard units, and so when ω_A is given in rad s^{-1}, the resistive torque is in N m.

List of symbols

a_c	centripetal acceleration
C_d	drag coefficient.
F	vector drag force
F_A	no. of video frames to complete a half rotation
F_D	no. of video frames to complete a full rotation
F_{drag}	drag force
FR	Fineness Ratio
g	acceleration of gravity
G	girth
I	moment of inertia
I_{total}	total moment of inertia
L	angular momentum
l	length
M_b	body mass
R	maximum radius
r	vector moment arm of **F**
t	time
v	tangential speed
v_s	swim speed
Δx	distance between any two points on the animal
Δx_B	distance between the pectoral fins and the dorsal fin, relevant to the stage B motion
Δx_C	distance between the dorsal fin and the flukes, relevant to the stage C motion
$\Delta\omega$	increase in angular speed due to the action of τ_{net}.
θ_o	initial angle
θ_R	rotational performance coefficient
ρ	density
τ	torque
τ_{net}	net torques acting over Δt
ω	angular speed
ω_A	initial angular speed

We would like to express our appreciation to Natural History New Zealand and specifically to Tracy Roe and Donald Ferns for supplying the dolphin video. We also thank Elizabeth Edwards, Susan Chivers and Bob Pitman for photographs and data of spinner dolphins and Moira Nusbaum for assistance with video analysis. This study was funded in part with grants from the Office of Naval Research to F.E.F.

References

Au, D. and Weihs, D. (1980). At high speeds dolphins save energy by leaping. *Nature* **284**, 548-550.

Au, D. and Perryman, W. (1982). Movement and speed of dolphin schools responding to an approaching ship. *Fish. Bull.* **80**, 371-379.

Cressey, R. F. and Lachner, E. A. (1970). The parasitic copepod and life history of diskfishes (Echeneidae). *Copeia* **1970**, 310-318.

Edel, R. K. and Winn, H. E. (1978). Observations on underwater locomotion and flipper movement of the humpback whale *Megaptera novaeangliae*. *Mar. Biol.* **48**, 279-287.

Fertl, D. and Landry, A. M., Jr (1999). Sharksucker (*Echeneis naucrates*) on a bottlenose dolphin (*Tursiops truncatus*) and a review of other cetacean-remora associations. *Mar. Mamm. Sci.* **15**, 859-863.

Fish, F. E. (2002). Balancing requirements for stability and maneuverability in cetaceans. *Integr. Comp. Biol.* **42**, 85-93.

Fish, F. E., Peacock, J. E. and Rohr, J. J. (2003). Stabilization mechanism in swimming odontocete cetaceans by phased movements. *Mar. Mamm. Sci.* **19**, 515-528.

Frohlich, C. (1980). The physics of somersaulting and twisting. *Sci. Am.* **242**, 154-164.

Guerrero-Ruis, M. and Urbán, J. R. (2000). First report of remoras on killer whales (*Orcinus orca*) in the Gulf of California, Mexico. *Aqu. Mamm.* **26**, 148-150.

Hester, F. J., Hunter, J. R. and Whitney, R. R. (1963). Jumping and spinning behavior in the spinner porpoise. *J. Mamm.* **44**, 586-588.

Hoerner, S. F. (1965). *Fluid-Dynamic Drag*. Brick Town (NJ): Published by author.

Hui, C. (1989). Surfacing behavior and ventilation in free-ranging dolphins. *J. Mamm.* **70**, 833-835.

Kolchin, S. and Bel'kovich, V. (1973). Tactile sensitivity in *Delphinus delphis*. *Zool. Zh.* **52**, 620-622.

Leatherwood, S., Reeves, R. R., Perrin, W. F. and Evans, W. E. (1988). *Whales, Dolphins, and Porpoises of the Eastern North Pacific and Adjacent Arctic Waters: A Guide to Their Identification*. New York: Dover Publications.

Moyle, P. B. and Cech, J. J., Jr (1988). *Fishes: An Introduction to Ichthyology*. Englewood Cliffs: Prentice Hall.

Norris, K. S. and Dohl, T. P. (1980). Behavior of the Hawaiian spinner dolphin, *Stenella longirostris*. *Fish. Bull*. **77**, 821-849.

Norris, K. S., Würsig, B., Wells, R. S. and Würsig, M. (1994). *The Hawaiian Spinner Dolphin*. Berkeley: University of California Press.

O'Toole, B. (2002). Phylogeny of the species of the superfamily Echeneoidea (Perciformes: Carangoidei: Echeneidae, Rachycentridae, and Coryphaenidae), with an interpretation of echeneid hitchhiking behaviour. *Can J. Zool*. **80**, 596-623.

Palmer, E. and Weddell, G. (1964). The relationship between structure, innervation and function of the skin of the bottle nose dolphin (*Tursiops truncatus*). *Proc. Zool. Soc. Lond.* **143**, 553-568.

Perrin, W. F. (2002). Spinner dolphin *Stenella longirostris*. In *Encyclopedia of Marine Mammals* (ed. W. F. Perrin, B. Würsig and J. G. M. Thewissen), pp. 1174-1178. San Diego: Academic Press.

Perrin, W. F. and Gilpatrick, J. W., Jr (1994). Spinner dolphin *Stenella longirostris* (Gray, 1828). In *Handbook of Marine Mammals*, Vol. 5, *The First Book of Dolphins* (ed. S. H. Ridgway and R. Harrison), pp. 99-128. San Diego: Academic Press.

Potter, M. C. and Foss, J. F. (1975). *Fluid Mechanics*. New York: Ronald Press.

Pryor, K. and Norris, K. S. (1991). *Dolphin Societies: Discoveries and Puzzles*. Berkeley: University of California Press.

Ridgway, S. H. and Carder, D. A. (1990). Tactile sensitivity, somatosensory responses, skin vibrations, and the skin surface ridges of the bottle-nose dolphin, *Tursiops truncatus*. In *Sensory Abilities of Cetaceans* (ed. J. Thomas and R. Kastelein), pp. 163-179. New York: Plenum Press.

Ridgway, S. H. and Carder, D. A. (1993). Features of dolphin skin with potential hydrodynamic importance. *IEEE Conf. Eng. Med. Biol*. **12**, 83-88.

Ritter, E. K. (2002). Analysis of sharksucker, *Echeneis naucrates*, induced behavior patterns in the blacktip shark, *Carcharhinus limbatus*. *Envir. Biol. Fish*. **65**, 111-115.

Ritter, E. K. and Godknecht, A. J. (2000). Agonistic displays in the blacktip shark (*Carcharhinus limbatus*). *Copeia* **2000**, 282-284.

Ritter, E. K. and Brunschweiler, J. M. (2003). Do sharksuckers, *Echeneis naucrates*, induce jump behaviour in blacktip sharks, *Carcharhinus limbatus*? *Mar. Freshw. Behav. Physiol*. **36**, 111-113.

Rommel, S. A. and Reynolds, J. E., III (2002). Skeletal anatomy. In *Encyclopedia of Marine Mammals* (ed. W. F. Perrin, B. Wursig and J. G. M. Thewissen), pp. 1089-1103. San Diego: Academic Press.

Slijper, E. J. (1962). *Whales*. Ithaca: Cornell University Press.

Streeter, V. L. (1966). *Fluid Mechanics*, 4th Edn. New York: McGraw-Hill.

Townsend, C. H. (1915). The power of the shark-sucker's disk. *Zool. Soc. Bull.* **18**, 1281-1283.

Webb, P. W. (1975). Hydrodynamics and energetics of fish propulsion. *Bull. Fish. Res. Bd. Can*. **190**, 1-158.

Weihs, D. (2002). Dynamics of dolphin porpoising revisited. *Integr. Comp. Biol.* **42**, 1071-1078.

Weihs, D. (2004). The hydrodynamics of dolphin drafting. *J. Biol.* **3**, 8.1-8.16.

Winn, H. E. and Reichley, N. E. (1985). Humpback whale *Megaptera novaeangliae* (Borowski, 1781). In *Handbook of Marine Mammals*, Vol. 3, *The Sirenians and Baleen Whales* (ed. S. H. Ridgway and R. Harrison), pp. 241-273. London: Academic Press.